Journal of Power Sources 237 (2013) 270–276

Contents lists available at SciVerse ScienceDirect

Journal of Power Sources

journal homepage: www.elsevier.com/locate/jpowsour

Polyvinylpyrrolidone–$LiClO_4$ solid polymer electrolyte and its application in transparent thin film supercapacitors

Jorge Rodríguez [a], Elena Navarrete [a], Enrique A. Dalchiele [b], Luis Sánchez [c], José Ramón Ramos-Barrado [a], Francisco Martín [a,*]

[a] Laboratorio de Materiales y Superficies (Unidad asociada al CSIC), Departamentos de Física Aplicada & Ingeniería Química Facultad de Ciencias, Campus de Teatinos, Universidad de Málaga, 29071 Málaga, Spain
[b] Instituto de Física & CINQUIFIMA, Facultad de Ingeniería, Herrera y Reissig 565, C.C. 30, 11000 Montevideo, Uruguay
[c] Departamento de Química Inorgánica e Ingeniería Química, Facultad de Ciencias, Campus de Rabanales, Edificio Marie Curie, Universidad de Córdoba, Spain

HIGHLIGHTS

- The conductivity of PVP depends on the concentration of $LiClO_4$.
- PVP–$LiClO_4$ layers exposed to air were characterized by ATR and TGA-DSC.
- A residual amount of ethanol preserves a good ionic conductivity.
- It was made a transparent glass/ITO/PEDOT/PVP–$LiClO_4$/PEDOT/ITO/glass capacitor.
- It was studied the effect of the aging time on the performance of the capacitor.

GRAPHICAL ABSTRACT

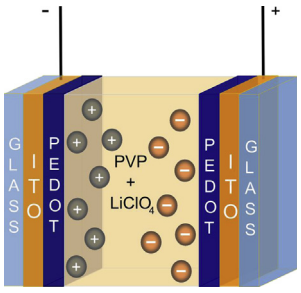

ARTICLE INFO

Article history:
Received 26 October 2012
Received in revised form
25 December 2012
Accepted 12 March 2013
Available online 21 March 2013

Keywords:
Polymer electrolyte
Polyvinylpyrrolidone
Supercapacitor
Transparent electrochemical devices

ABSTRACT

Films of PVP (polyvinylpyrrolidone) and $LiClO_4$ have been obtained by dip coating to be used as solid ionic conductors in transparent energy storage systems. The dependence of the ionic conductivity of PVP/$LiClO_4$ films on temperature, lithium salt concentration, and residual solvent content or humidity has been studied. The films were used in a symmetrical supercapacitor (PEDOT/PVP/PEDOT). Whose behaviour with the aging time was analysed as well. It was observed that the experimental differences in the performance of a lithium ion based energy storage devices using these films as solid electrolyte may be due to changes in the residual content of the solvent used in their preparation or the hygroscopic nature of the electrolyte.

1. Introduction

In recent years, solid polymer electrolytes have become very important as key materials for different electrochemical devices, such as rechargeable batteries [1–3], electrochromic displays [1], and supercapacitors [1]. Solid polymer electrolytes are compounds formed through the dissolution of salts into polar and high-molecular weight macromolecules that can interact strongly with cations. Lithium ion conductive materials are particularly attractive owing to their applications as a solid polymer electrolyte for lithium rechargeable batteries [3] and other solid-state electrochemical devices [3]. Hence, lithium salt-based electrolytes have

* Corresponding author. Departamento de Ingeniería Química, Universidad de Málaga, 29071 Málaga, Spain. Tel.: +34 952 132037; fax: +34 952 132382.
E-mail address: marjim@uma.es (F. Martín).

0378-7753/$ – see front matter © 2013 Elsevier B.V. All rights reserved.
http://dx.doi.org/10.1016/j.jpowsour.2013.03.043

been the focus of a wide variety of fundamental and application-oriented studies [4].

To reduce costs and to extend the useful lifetime of a device, it is necessary to obtain a solid polymer electrolyte with good stability during electrochemical cyclation under environmental conditions. For most potential applications, it is desirable that the solid polymer electrolytes display a reasonable ionic conductivity (over 10^{-4} S cm^{-1}) [5]. It must be pointed out that the ionic conductivity of solid polymer electrolytes is dependent on the inorganic salt to polymer molar ratio, and on the nature of the lithium salt, due to the transfer efficiency of charge carriers and complex formation between the metal cation and polymer [6]. Moreover, the presence of any residual solvent has an influence on the conductivity [7].

Within the vast variety of polymer electrolytes, polyvinylpyrrolidone (PVP) has been the focus of a wide range of fundamental and application-orientated studies [1,2,5,8,9]. PVP is an amorphous polymer with good stability, which has the aspect of a white powder [4]. It can easily be processed, and it displays moderate ionic conductivity, i.e.: associated with PVA (polyvinyl alcohol) it is about 4.6×10^{-7} S cm^{-1} at room temperature [10]. PVP exhibits a high transition temperature value, T_g, around 170 °C because of the presence of its rigid pyrrolidone groups, but water can act as a plasticizer lowering this T_g value from approximately 170 °C to below 40 °C [11]. PVP is a polymeric lactam with an internal amide bond, and the tertiary amide carbonyl groups of PVP posses a marked Lewis base character such that PVP can form a variety of complexes with a wide range of inorganic salts. It is also hygroscopic and easily soluble in water and organic solvents such as alcohols [12]. Due to these characteristics, layers of PVP can be easily obtained by a dip-coating process or by other similar low cost techniques carried out under air atmosphere conditions. However, by using these thin film growth methods the influence of the air atmosphere parameters (i.e.: ambient humidity), on the properties (i.e.: ionic conductivity) of the PVP layers obtained must be taken into account. In fact, the properties of the PVP layers obtained could change when exposed to air environmental conditions, due to: i) additional loss of residual solvent, and ii) by incorporating environmental humidity. Therefore, some differences in the behaviour of lithium batteries or supercapacitor devices using PVP as the solid electrolyte could be explained by changes caused by the residual presence of solvent used in its preparation or humidity in the solid polymer electrolyte due to the hygroscopic nature of the PVP.

Regarding polymer electrolytes based on PVP doped with lithium perchlorate ($LiClO_4$) salt, PVP–$LiClO_4$, there is very little information in the literature [4], and to our knowledge, there are no reports of conductivity studies on the PVP–$LiClO_4$ solid polymer electrolyte. In view of the above, the present paper aims mainly to report on the ionic conductivity of the PVP–$LiClO_4$ solid polymer electrolyte system as a function of the lithium perchlorate content. Moreover, transparent electronics (i.e.: transparent diodes, functional windows, TFT, CMOS, etc.), are an emerging and promising technology for the next generation of optoelectronic devices [13]. As such, the possibility of growing transparent solid polymer electrolytes provides the opportunity to fabricate transparent electrochemical storage systems, with great relevance for application in transparent electronics. PVP has attracted special attention amongst the conjugated polymers because of its good environmental stability, easy processing and excellent transparency [14].

On the other hand, supercapacitors, also known as electrochemical capacitors, have attracted recently great attention due to their high power density and long term cycles [15,16]. In general, they can be classified into two categories in terms of their energy storage mechanism, i.e.: electric double layer capacitors (EDLCs) and pseudo-capacitors [15,17]. EDLC type devices generate capacitance from charge separation at the electrode/electrolyte interface, while the pseudo-capacitance type generates capacitance from fast faradic reactions in the electrode material [17]. The EDLC is an intermediate power/energy storage/supply device that can provide a higher energy density than a conventional electrostatic capacitor, a higher power density than batteries, as well as a much longer cycle life [15,18].

In the present study, the dependence of the ionic conductivity of dip-coated PVP–$LiClO_4$ solid electrolyte thin films on temperature, lithium salt concentration, aging time, and residual solvent or humidity content has been studied. Moreover, these films have been employed in the fabrication of a symmetrical electrochemical supercapacitor (PEDOT/PVP–$LiClO_4$/PEDOT), which to our knowledge, is the first time that a supercapacitor of this type has been reported in the literature. The aging time effect on the behaviour of the proposed supercapacitor has also been studied. Moreover, all components of these devices have been fabricated as transparent thin films.

2. Experimental

2.1. Materials

Polyvinyl pyrrolidone (PVP) with a molecular weight of 1,300,000, lithium perchlorate ($LiClO_4$) and (3,4-ethylene dioxythiophene) EDOT monomer were purchased from Aldrich, USA. All chemicals were used as received without any further treatment. Commercial In_2O_3:Sn (ITO) thin films (8–10 Ω Sq^{-1}) on glass were used as substrate electrodes.

2.2. Preparation of PVP–$LiClO_4$ solid electrolyte thin films

Solutions of PVP–$LiClO_4$ were prepared by dissolving desired amounts of PVP and lithium salt in ethanol. Immediately after continuous stirring during 30 min at room temperature, the polymer electrolyte was cast forming films using the dip coating technique over copper circle substrates of 13 mm in diameter and 0.124 mm in thickness. The copper substrates were previously ultrasonically cleaned for 10 min with isopropanol and afterwards for 10 min with acetone. Then the copper substrates were dipped into the PVP-ethanol-$LiClO_4$ solution and withdrawn at a speed of 180 mm min^{-1}. Between each dipping, the samples were dried with a halogen lamp (50 °C), for 10 min. This procedure was carried out inside a dry-box with a partial vacuum, and the air purged with a nitrogen stream. The film thickness of each PVP–$LiClO_4$ layer was estimated by scanning electron microscopy (SEM) cross sectional images.

2.3. Measurement of ionic conductivity of PVP–$LiClO_4$ solid electrolyte thin films

Ionic conductivities of the (PVP–$LiClO_4$) solid polymer electrolyte films were measured using an AC impedance technique with an HP Impedance Analyzer, where the AC frequency was scanned from 5×10^6 Hz to 1 Hz at a voltage amplitude of 250 mV, and temperature range 273–333 K. From the resulting complex impedance plots the bulk resistance of the polymer electrolyte was obtained. Ionic conductivity of the solid polymer electrolyte was calculated from the measured bulk resistance, area and thickness of the polymer thin film, by using the following equation:

$$\sigma = L/(R_b A) \quad (1)$$

where L is the thickness of the polymer electrolyte (cm), A is the area of the blocking electrode (cm^2), and R_b is the bulk resistance of the polymer electrolyte.

To study the effect of the aging time on conductivity, PVP–$LiClO_4$ samples were left in air at room temperature from 6 to 72 h after being made before DTGA measurements were carried out.

2.4. Thermal analysis

Thermogravimetric analysis (TGA) and Differential Scanning Calorimetry (DSC) data were recorded on an SDT-Q600 analyzer from TA Instruments. The temperatures varied from room temperature (25 °C approx.) to 145 °C at a heating rate of 5 °C min^{-1}. Measurements were carried out on samples in open platinum crucibles under air flow.

2.5. ATR analysis

Attenuated Total Reflectance (ATR) spectra were obtained using a Golden Gate Single Reflection Diamond ATR System using a Fourier Transformed IR Vertex-70. Transmittance measurements were carried out with a spectrometer VARIAN Cary 5000.

2.6. Supercapacitor fabrication

In order to evaluate the performance of the PVP–$LiClO_4$ solid polymer electrolyte, symmetrical structured electrochemical double layer capacitors (EDLCs): glass/ITO/PEDOT/PVP–$LiClO_4$/PEDOT/ITO/glass were fabricated. In a first step, PEDOT (poly(3,4-ethylenedioxythiophene)) thin films were grown by electropolymerization of EDOT over commercial ITO/glass substrates. To this end, a typical three electrode electrochemical cell geometry was used, comprising an ITO-coated glass substrate (2.0 cm^2), a Pt wire and a saturated calomel electrode (SCE) ($E = +0.25$ V vs. normal hydrogen electrode (NHE)), as working, counter and reference electrodes, respectively. The electrodeposition bath consisted of an aqueous solution of 3 mM EDOT + 0.2 M $LiClO_4$. All solutions were prepared from analytical grade reagents and 18.3 MΩ cm Millipore water. The electrodeposition was performed at room temperature. Nitrogen was flushed through the cell and the electrolyte prior to the experiments, and a nitrogen flow was maintained over the solution during the electrodeposition process. The substrates were first cleaned ultrasonically, 5 min in acetone, 5 min in ethanol and 5 min in DI water. The PEDOT thin film was grown by a potential cycling procedure between −0.8 and 2 V at 75 mV s^{-1}, for 5 cycles using an Autolab PGSTAT30 potentiostat/galvanostat as reported in our earlier work [19]. Briefly, the electropolymerization process involves oxidation of EDOT molecule at the electrode surface [20–26] and its subsequent polymerization, according to the following processes [25,26]:

$$n\mathrm{EDOT}\left(\mathrm{sol}\right) \rightarrow n\mathrm{EDOT}^{+\bullet} + ne^{-} \quad (2)$$

$$n\mathrm{EDOT}^{+\bullet} + z\mathrm{ClO_4}^{-} \rightarrow \left(n-z\right)\mathrm{H}++\left[(\mathrm{EDOT}_n)^{z+}\mathrm{ClO_4}^{-}{}_z\right] \quad (3)$$

where *n*e- are *n*-electrons, *n*EDOT are n-monomers of 3,4-ethylenedioxythiophene, $n\mathrm{EDOT}^{+\bullet}$ are *n*-radical cations of EDOT and *z* is a measure of the doping level of polymer.

In a second step, a PVP–$LiClO_4$ solid polymer thin film was grown by the dip-coating technique (as mentioned above in Section 2.2), onto a previously synthesized glass/ITO/PEDOT. In a third step, the freshly prepared glass/ITO/PEDOT/PVP–$LiClO_4$ sample was fastened to a glass/ITO/PEDOT sample by simple hand pressure. Several glue fixing points were applied to the interface to ensure mechanical stability.

2.7. Supercapacitor performance study

The performance of the resulting supercapacitor devices was evaluated by cyclic voltammetry carried out with an Autolab PGSTAT30 potentiostat. It is worth noting that the data presented here in the performance studies of the EDLC were obtained from a two-electrode cell test and not from the widely used three-electrode type that overestimates the results [18,27]. In fact, it as has been reported in the literature that the results should be quadrupled compared with the three-electrode cell tests [18,27].

2.8. Scanning electron microscopy characterization

The cross section morphology of the fabricated supercapacitors was studied by scanning electron microscopy (SEM) in the back-scattered mode (BSE), with a JEOL JSM-840 microscopy.

3. Results and discussion

3.1. Ionic conductivity study

The effect of lithium perchlorate salt content on the ionic conductivity of PVP–$LiClO_4$ samples was studied, and the results are depicted in Fig. 1a. It can be seen that ionic conductivity increases as the amount of lithium perchlorate increases, reaching a maximum of ionic conductivity as the $LiClO_4$/PVP weight ratio

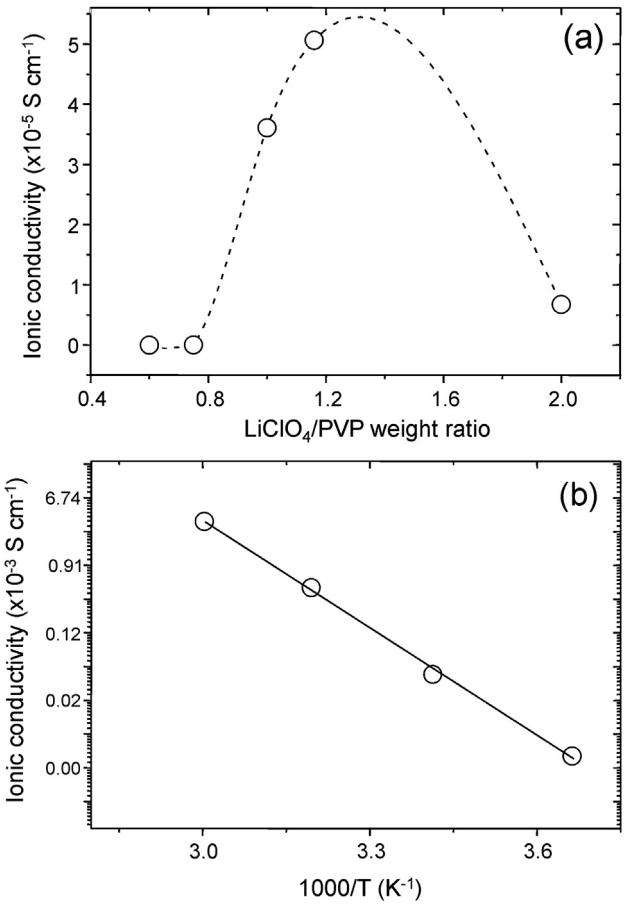

Fig. 1. (a) Ionic conductivity as a function of the lithium perchlorate content in a typical PVP–$LiClO_4$ sample measured at room temperature (Solid line is a guide for the eye). (b) Plot of the temperature dependence of ionic conductivity for a sample with a $LiClO_4$/PVP weight ratio of 1.2, where the linear fitting is indicated by a dashed line.

attains a value of 1.2. Beyond this point the ionic conductivity decreases with increasing lithium perchlorate content. A similar trend has been observed by Zhou et al. [6] when doping a poly(-organophosphazene) polymer with $LiClO_4$. In the latter case a maximum value on the ionic conductivity was reached for a lithium content of 14%. When the $LiClO_4$ concentration increases, an increase of the ionic conductivity is expected due to the increase of charge carrier numbers in the polymer electrolyte. On the other hand, the decrease of the ionic conductivity of the polymer electrolyte at high $LiClO_4$ contents could be due to the polymer cages trapping liquid electrolyte, becoming smaller and thus hindering ionic motion. Also, at high lithium salt concentration ranges the decreasing conductivity could be due to emerging salt crystallites as a result of having exceeded the local solubility of the lithium salt in the polymer. Excessive cations and anions could aggregate and form crystalline phases that block the movement of the charge carrier, which would result in a decrease in the ionic conductivity of the polymer electrolyte [28,29,30]. Solvent loss at higher salt electrolyte concentrations could lead to a local increase in the concentration of $LiClO_4$ and crystallization of $LiClO_4$ in the PVP matrix. This solvent loss would reduce the ion mobility in the polymer. In our case, the PVP layers were heated at 50 °C between dip cycles, as described in the experimental section. However, after drying, a small fraction of the initial ethanol remains in the PVP and if the PVP/$LiClO_4$ film is exposed to an ambient temperature, it can lose some more of the initial content of residual ethanol. However, because of the hygroscopic nature of the PVP, it could gain water.

Fig. 1b shows the variation in the logarithm of the ionic conductivity with the inverse absolute temperature for a typical PVP–$LiClO_4$ sample with a $LiClO_4$/PVP weight ratio of 1. From the plot, it is evident that as the temperature increases the ionic conductivity increases, reaching its highest value of 3.34×10^{-3} S cm^{-1} at value at 60 °C. Moreover, the regression value of the plot using a linear fit is found to be close to unity suggesting that the temperature dependent ionic conductivity obeys an Arrhenius relationship. The dependence of the PVP–$LiClO_4$ ionic conductivity on temperature would be owing to the fact that the polymer matrix is amorphous and has large numbers of free-volume cages. This number increases with increasing temperature just as described in the free-volume model [31]. This results in an increase in movable ions and higher ionic conductivity of PVP at ambient conditions [32]. The activation energy was calculated from the logarithm of the ionic conductivity versus $1/T$ plot of Fig. 1b using the Arrhenius equation:

$$\sigma = \sigma_0 \exp(-E_a/(kT)) \quad (4)$$

where σ_0 is a constant, E_a, the activation energy, k, the Boltzmann constant and T the absolute temperature. An activation energy value of 88.39 kJ mol^{-1} (0.92 eV) was calculated.

3.2. ATR and TGA–DSC discussion

Due to its hygroscopic nature PVP takes up ambient moisture when it is exposed to an air atmosphere. When absorbed onto PVP, water molecules are linked to the PVP C=O groups by hydrogen bonds. Every C=O group can be directly linked to two water molecules via these bonds [32]. The presence of water in PVP is a limitation to the voltage window because at 1.3 V the water is oxidized. In Fig. 2a, curve 1 shows the ATR region of the PVP powder from 3000 cm^{-1} to 4000 cm^{-1} after being exposed for days to non saturated air. The observed bands correspond to –OH bonds (3000 cm^{-1} to 3600 cm^{-1}) and the C–H stretching 2700 to 3030 cm^{-1} with asymmetrical and symmetrical C–H stretching vibrations at around 2962 cm^{-1} and 2872 cm^{-1} respectively. The fundamental stretching and in-plane bending mode of water

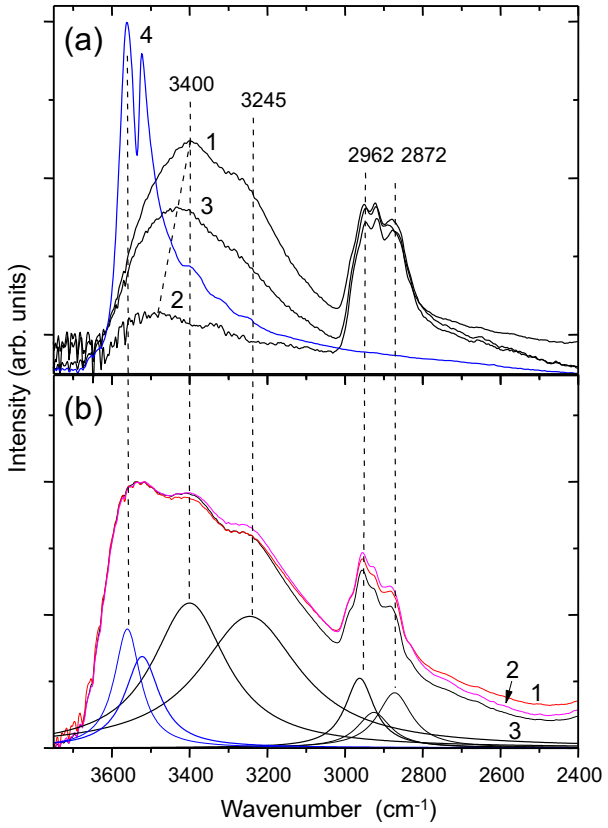

Fig. 2. ATR spectra. (a) a-1 PVP powder after exposure to air, a-2 after heating at 100 °C for 1 h, a-3 after heating at 100 °C and exposed to air for 10 min, a-4 pure solid $LiClO_4$. (b) $LiClO_4$/PVP films (weight ratio equal to 1) on glass after 24 (b-1), 48 (b-2) and 72 (b-3) hours of exposure to air after fabrication.

molecules occurs within the 3900–2800 cm^{-1} region at around 1640 cm^{-1}. Water displays a large band in the 3900–2800 cm^{-1} because O–H stretching modes of water are complex due to symmetric and antisymmetric coupling and to intermolecular and intramolecular hydrogen bonding of different strengths. Although the increasing intensity of the band at 3400 cm^{-1} with increasing water content is similar to the behaviour of other hydrophilic polymers, a difference is observed in this case; with respect to the also hydrophilic PVA [32], the 3400 cm^{-1} band is shifted to a higher wavelength when the water content decreases (Fig. 2a). When the PVP powder is exposed for days to non saturated air (Fig. 2a, curve 1) with an average relative humidity of 45%, and then dried at 100 °C for 1 h, the –OH bands from 3000 cm^{-1} to 3800 cm^{-1} were considerably reduced (Fig. 2a, curve 2). But after another 10 min exposure to the air (Fig. 2a, curve 3), an increase of the OH bands is observed due to water gain. A more prolonged exposure would lead to a limit in the water gained, and therefore the amount of water in the PVP after exposure to air for days could be considered to have reached this limit. The limiting amount of water gained has been estimated by TGA to be 8% of the total initial weight (Fig. 4a). Because the intensity of the –CH stretching bands remains nearly constant (Fig. 3a), the relationship between the –OH and –CH intensities in this region could be used to estimate the water content of the PVP. Fig. 3a also compares the ATR-FTIR of pure solid $LiClO_4$. In the 2600 to 3000 cm^{-1} range, $LiClO_4$ displays two bands at 3560 cm^{-1} and 3525 cm^{-1}. Other distinctive bands for $LiClO_4$ appear around 1100 cm^{-1} due to Cl–O stretching. In this region PVP does not show any significant absorption bands. When $LiClO_4$ is added to the PVP, the $LiClO_4$ bands convolute with the –OH bands as shown in Fig. 3b.

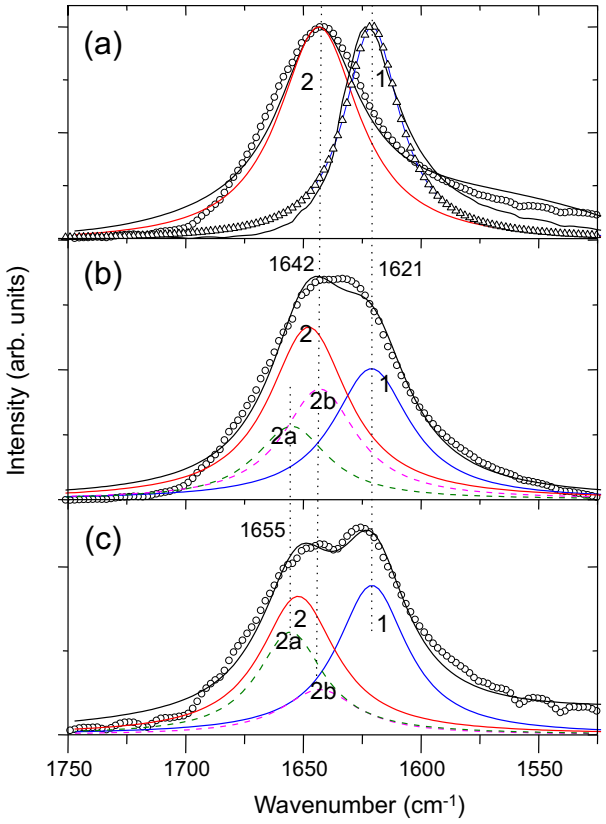

Fig. 3. ATR spectra. (a) PVP powder as received (a-2), pure solid $LiClO_4$ (a-1) and Lorentz fit. (b) $LiClO_4$/PVP films (weight ratio equal to 1) onto glass and deconvolution curves. (c) $LiClO_4$/PVP films (weight ratio equal to 2) onto glass and deconvolution curves.

The bands corresponding to the pure PVP carbonyl stretching band (1642 cm^{-1}) and pure $LiClO_4$ (1621 cm^{-1}) and the corresponding fit to a Lorentz function are shown in Fig. 3a. Fig. 3b and c shows the same region for the film with weight ratios of 1 and 2 $LiClO_4$/PVP respectively. Lithium and ClO_4^- form complexes with the C═O groups. As the $LiClO_4$ concentration increases, the carbonyl bands in Fig. 3(c) broaden gradually, and a new band appears at 1650 cm^{-1} as a result of the coordination between the Li^+ and the oxygen atom on the carbonyl group of the PVP. In addition to the free carbonyl band, the carbonyl stretching band of PVP shifts to a lower frequency (1640 cm^{-1} to 1650 cm^{-1}) as a consequence of the coordination between the Li^+ cation and the oxygen atom on the carbonyl group of the PVP as proposed by W. Hew-Der and Chun-Yi et al. [4,5]. The deconvolution of the peaks in the infrared spectral regions analysed was made by using the best fit with Lorentzian functions. The C═O stretching band for PVP at 1640 cm^{-1} and $LiClO_4$ at 1620 cm^{-1} convolute to give a unique band. However this band can be deconvoluted into three peaks, corresponding to $LiClO_4$ at 1620 cm^{-1}, free C═O PVP at 1640 cm^{-1}, and at 1655 cm^{-1} for C═O associated with Li^+ ions by forming a polymer–salt complex. When the amount of $LiClO_4$ increases, then the peak at 1655 cm^{-1} increases, showing that more C═O groups are forming complexes with Li^+ ions, Fig. 2b and c.

To study the effect of exposure to air of the solid electrolyte, electrolyte films with a $LiClO_4$/PVP weight ratio of 1 were deposited onto glass by dip coating and exposed to non saturated air from 6 to 72 h. These films had been dried at 50 °C for 15 min previous to their exposure to air during the dip coating process. ATR spectra and TGA measurements, Figs. 2 and 4 respectively, were carried out immediately upon the exposure time ending. The IR regions from 2500 cm^{-1} to 4000 cm^{-1} for these films are shown in Fig. 2, in which it can clearly be seen that the band intensities from 2400 cm^{-1} to 4000 cm^{-1} are identical for all the films exposed from 24 to 72 h. The weight loss percentages at temperatures higher than 80 °C are also similar (Fig. 4a) for these films at around 12%. However the sample exposed for 6 h shows a bigger weight loss of 17%, which could be due to a greater amount of residual ethanol in the polymer film, and the conductivity of this film is the highest (Fig. 4b), being 1.89×10^{-4} S cm^{-1} for the 6-h sample and 3.29×10^{-6} S cm^{-1} for the 24-h sample. The samples exposed to the atmosphere from 24 to 72 h are poorly conductive (Fig. 4b). Fig. 4a also shows the DSC curves. The DSC curves for 6 h and 24 h show an endothermic peak related with loss of volatile, with a maximum (minimum in the figure) around 37 °C and end at 70 °C. The endothermic peak shrinks for the sample with higher time of exposition, showing that a less residual amount of ethanol has stayed in the PVP layer after 24 h comparatively to 6 h. For pure PVP powder exposed to air, which has gained some moisture, the endothermic peak extends to higher temperatures showing the maximum at 59 °C and end at 100 °C. This change of temperature of the endothermic peak is related with the higher vapour pressure of the ethanol comparatively to water.

3.3. Supercapacitor device fabrication and characterization

In order to study the performance of the PVP–$LiClO_4$ as a solid polymer electrolyte in transparent electrochemical devices, symmetrical structured electrochemical double layer capacitors (EDLCs): glass/ITO/PEDOT/PVP–$LiClO_4$/PEDOT/ITO/glass were

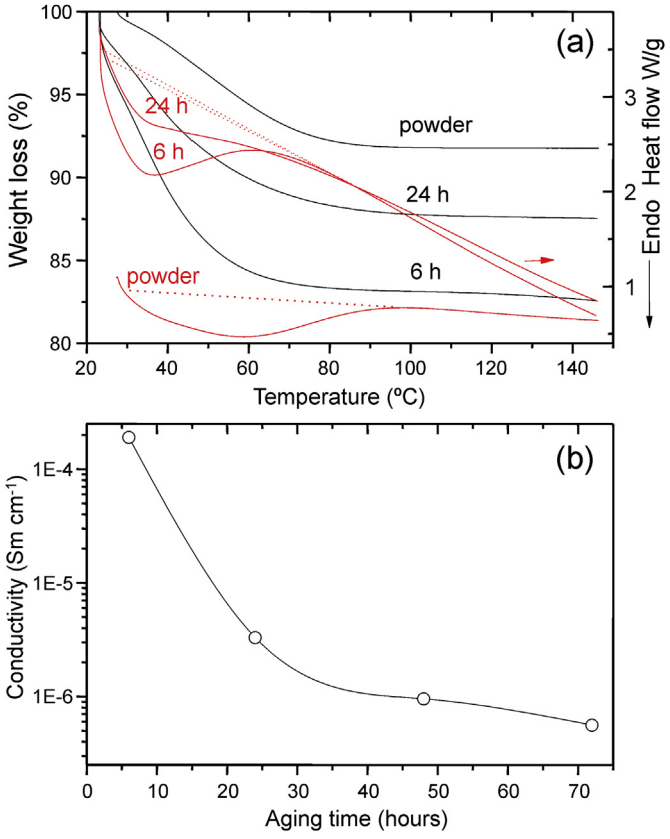

Fig. 4. (a) TGA weight loss and DSC curves for PVP powder as received after air exposure and $LiClO_4$/PVP films (weight ratio equal to 1) on glass after 6 and 24 h of air exposure after fabrication.

fabricated. A scheme of the device is depicted in Fig. 5a. A SEM image of the cross-sectional view of a supercapacitor made in our laboratory is shown in Fig. 5b. In this image all the layers constituting the supercapacitor can be seen, except the ITO layers, as they are too thin (ca. 150 nm). Due to the effect that the thickness exerts on the capacitance, different thicknesses of the PVP–$LiClO_4$ solid polymer electrolyte layer (controlled by the number of dip-coating cycles), have been assayed, in all cases with a $LiClO_4$/PVP weight ratio of 1. It must be pointed out that each dip coating cycle corresponds to approximately 15 μm of layer thickness. It is found that the electrochemical response of the supercapacitor is influenced by the PVP–$LiClO_4$ electrode's thickness. Fig. 6a shows the resulting cyclic voltammetry (CV) curves (scan rate of 75 mV s^{-1}) for four different PVP–$LiClO_4$ electrode layer numbers (1–4 dip cycles). All the CV curves shown in Fig. 6a have a nearly rectangular shape, indicating a nearly ideal capacitive response. Moreover, it can be seen that the specific electrode capacitance reaches a maximum of mass specific capacitance (15 F g^{-1}) when the number of layers is two. The effect of the PVP–$LiClO_4$ electrode layer numbers on the CV behaviour of the supercapacitor can be explained as follows. Dielectric breakdown could cause current leakage between the electrodes when the thickness of the polymer is low; in fact, the external circuit intensity recorded by the potentiostat is one order of magnitude lower for 15 μm of thickness with respect to the

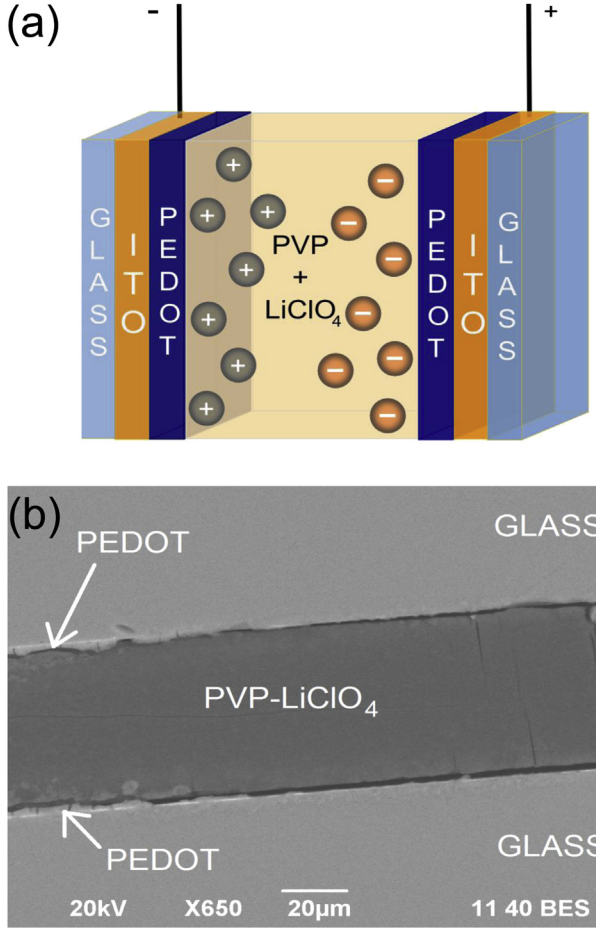

Fig. 5. (a) Scheme of the glass/ITO/PEDOT/PVP–$LiClO_4$/PEDOT/ITO/glass symmetrical structured electrochemical double layer capacitor device. (b) BSE–SEM cross-sectional view of the supercapacitor. ITO layers are not appreciable due to their very small thickness.

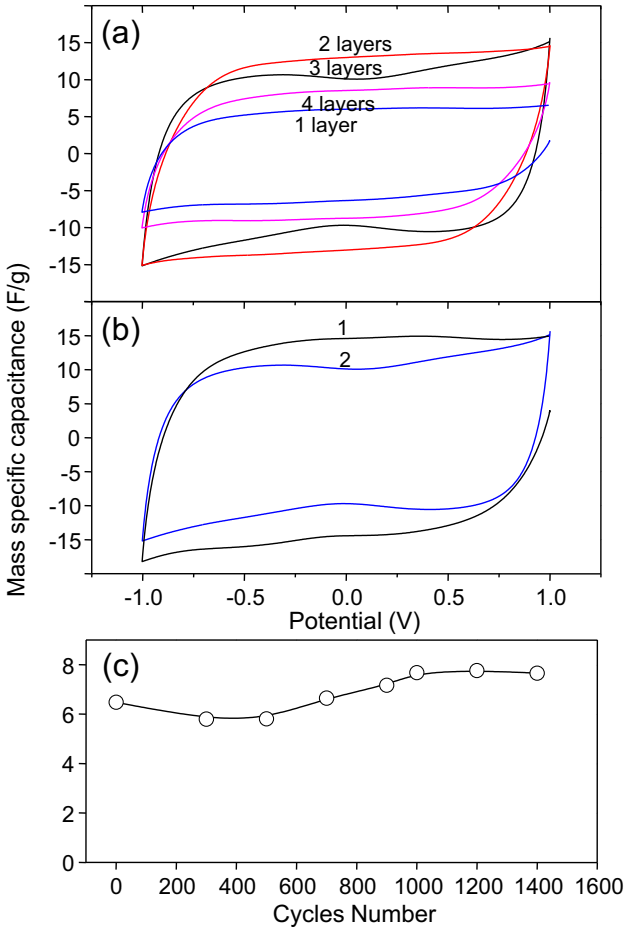

Fig. 6. (a) Cyclic voltammograms of the capacitor depicted in Fig. 5a, for different PVP–$LiClO_4$ solid polymer electrolyte layer numbers. (b) Cyclic voltammograms of a capacitor as depicted in (a), with two PVP–$LiClO_4$ solid polymer layers, recorded just after the device has been prepared (curve 1), and recorded after an aging time of nine months (curve 2). (c) Mass specific capacitance over 1400 cycles of cyclic voltammetry for a nine month aged supercapacitor assayed in (b) (the solid line is a guide for the eye). In all cases the $LiClO_4$/PVP weight ratio was 1, and the cyclic voltammetry scan rate was 100 mV s^{-1}.

others. The capacitance of a parallel plate capacitor is inversely proportional to the distance separating the electrodes. When the thickness of the electrolyte increases, the transport of the electrolyte ions is hindered. On the other hand, as discussed above, the conductivity of the polymer depends on the amount of residual solvent in the polymer electrolyte. An undesirable effect due to the loss of residual solvent could be the shrinking of the polymer electrolyte leading to local contact being lost with the surface of the electrodes or polymer electrolyte cracking. Owing to this, an important aspect for any material to be used as a supercapacitor electrolyte is its behaviour after a certain aging time, and the electrochemical stability after repeated charge/discharge cycling. Fig. 6b shows a comparison of the characteristic CV curves for a supercapacitor device (with two layers of PVP–$LiClO_4$), taken just after the device has been prepared, and after the device has been stored under air atmosphere conditions and at room temperature after nine months aging time. Very little difference between the two CV profiles can be seen, indicating a very small decrease in the mass specific capacitance from 15 to 10 F g^{-1} after a nine month aging time (see Fig. 6b). Furthermore, when a cyclability study was carried out by cyclic voltammetry of the supercapacitor device with four layers (four dip cycles) after nine months storage in an air atmosphere, a decrease of 10% of specific capacitance was found at

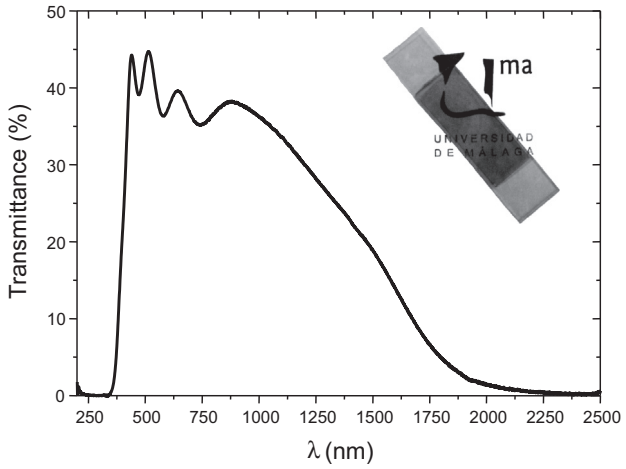

Fig. 7. Optical transmittance spectra of a typical glass/ITO/PEDOT/PVP–$LiClO_4$/PEDOT/ITO/glass symmetrical structured electrochemical double layer capacitor device. The inset shows a photograph of the supercapacitor device to illustrate its level of transparency.

the early 500 cycles stage (scan rate 100 mV s^{-1}), but after the 500 cycles stage the specific capacitance increases significantly with the increasing cycle number, until the capacitance reaches a plateau, and the values before aging are recovered (Fig. 6c).

3.4. Optical transmittance analysis

Light transmittance of the supercapacitor can be seen in Fig. 7, in which the transmittance spectrum of an EDLC device is shown (see Fig. 5), which reaches its maximum value of almost 50% in the visible wavelength region, from 370 to 770 nm.

4. Conclusions

Films of solid polymer electrolyte consisting of mixtures of polyvinylpyrrolidone (PVP) and $LiClO_4$ with various mass ratios were synthesized by the dip-coating method. The ionic conductivity increases with temperature reaching a value of 3.34×10^{-3} S cm^{-1} at 60 °C for a $LiClO_4$/PVP weight ratio equal to 1.2. At higher $LiClO_4$/PVP ratios the conductivity decreases. Dried PVP gains humidity quickly when it is exposed to an air atmosphere, reaching a constant weight increase of around 8%. The residual amount of ethanol is important for preserving a good ionic conductivity. The loss of ethanol reduces the ionic conductivity. It has been demonstrated that these films are available for use as a solid ionic polymer electrolyte in transparent supercapacitors. Their behaviour depends on the aging conditions of the electrolyte. A decrease in the mass specific capacitance is found when the electrolyte is aged under ambient conditions, but the mass specific capacitance is recovered after several hundred charge/discharge cycles.

Acknowledgements

The authors are grateful to MINECO of Spain, for the financial support received (Consolider Ingenio2010 FUNCOAT CSD2008-00023 and TEC2010-16700). E.A.D. thanks the support received from PEDECIBA-Física and CINQUIFIMA, Uruguay.

References

[1] M. Ravi, Y. Pavani, K. Kiran-Kumar, S. Bhavani, A.K. Sharma, V.V.R. Narasimha-Rao, Mater. Chem. Phys. 130 (2011) 442–448.
[2] N. Rajeswari, S. Selvasekarapandian, S. Karthikeyan, M. Prabu, G. Hirankumar, H. Nithya, C.J. Sanjeeviraja, Non-Cryst. Solids 357 (2011) 3751–3756.
[3] A. Sato, T. Okumura, S. Nishimira, H. Yamamoto, N. Ueyama, J. Power Sources 146 (2005) 423–426.
[4] W. Hew-Der, W. I-Der, C. Feng-Chih, Polymer 42 (2001) 555–562.
[5] C. Chun-Yi, Y. Ying-Jie, K. Shiao-Wei, C. Hsien-Wei, C. Feng-Chih, Polymer 48 (2007) 1329–1342.
[6] S. Zhou, S. Fang, Eur. Polym. J. 43 (2007) 3695–3700.
[7] O.V. Bushkova, V.M. Zhukovsky, B.I. Lirova, A.L. Kruglyashov, Solid State Ionics 119 (1999) 217–222.
[8] J. Qiao, J. Fu, R. Lin, J. Ma, J. Liu, Polymer 51 (2010) 4850–4859.
[9] Y.-W. Park, D.-S. Lee, J. Non-Cryst. Solids 351 (2005) 144–148.
[10] C.V. Subba, A.K. Sharma, V.V.R. Narasimha-Rao, J. Power Sources 111 (2002) 357–360.
[11] S. Fitzpatrick, J.F. McCabe, C.R. Petts, S.W. Booth, Int. J. Pharm. 246 (2002) 143–151.
[12] D.T. Turner, A. Schwartz, Polymer 26 (1985) 757–762.
[13] Y. Yang, S. Jeong, L. Hu, H. Wu, S.W. Lee, Y. Cui, Proc. Natl. Acad. Sci. 108 (2011) 13013–13018.
[14] K. Sivaiah, B. Hemalatha, S. Buddhudu, Indian J. Pure Appl. Phys. 48 (2010) 658–662.
[15] H. Zheng, J. Wang, Y. Jia, C. Ma, J. Power Sources 216 (2012) 508–514.
[16] Y.J. Kang, S.J. Chun, S.S. Lee, B.Y. Kim, J.H. Kim, H. Chung, S.Y. Lee, W. Kim, ACS Nano 6 (2012) 6400–6406.
[17] L. Lai, H. Yang, L. Wang, B.K. Teh, J. Zhong, H. Chou, L. Chen, W. Chen, Z. Shen, R.S. Ruoff, J. Lin, ACS Nano 6 (2012) 5941–5951.
[18] L. Basiricò, G. Lanzara, Nanotechnology 23 (2012) 305401–305413.
[19] J. Rodríguez, E. Navarrete, F. Martín, R. Schrebler, J.R. Ramos-Barrado, E.A. Dalchiele, Thin Solid Films 525 (2012) 88–92.
[20] S. Patra, N. Munichandraiah, J. Appl. Polym. Sci. 106 (2007) 1160–1171.
[21] C. Ocampo, R. Oliver, E. Armelin, C. Alemán, F. Estrany, J. Polym. Res. 13 (2006) 193–200.
[22] L. Pigani, A. Heras, A. Colina, R. Seeber, J. López-Palacios, Electrochem. Commun. 6 (2004) 1192–1198.
[23] E. Tamburri, S. Orlanducci, F. Toschi, M.L. Terranova, D. Passeri, Synth. Met. 159 (2009) 406–414.
[24] E. Nasybulin, S. Wei, M. Cox, I. Kymissis, K. Levon, J. Phys. Chem. C 115 (2011) 4307–4314.
[25] D.K. Taggart, Y. Yang, S.-C. Kung, T.M. McIntire, R.M. Penner, Nano Lett. 11 (2011) 125–131.
[26] F. Di Franco, P. Bocchetta, M. Santamaria, F. Di Quarto, Electrochim. Acta 56 (2010) 737–744.
[27] E. Raymundo-Piñero, V. Khomenko, E. Frackowiak, F. Béguin, J. Electrochem. Soc. 152 (2005) A229–A235.
[28] C.S. Ramya, S. Selvasekarapandian, T. Savitha, G. Hirankumar, P.C. Angelo, Phys. B Cond. Matter 393 (2007) 11–17.
[29] D.M. DeLongchamp, P.T. Hammond, Chem. Mater. 15 (2003) 1165–1173.
[30] T. Miyamoto, K.J. Shibayama, Appl. Phys. 44 (1973) 5372–5376.
[31] Z. Lan, J. Wu, D. Wang, S. Hao, J. Lin, Y. Huang, Sol. Energy 80 (2006) 1483–1488.
[32] Z.H. Ping, Q.T. Nguyen, S.M. Chen, J.Q. Zhou, Y.D. Ding, Polymer 42 (2001) 8461–8467.